Jordan Journal of Physics, Vol. 18, No 4, pp. 529-549 (2025).
https://jjp.yu.edu.jo/index.php/jjp/article/view/323. https://doi.org/10.47011/18.4.10

On the origin of cosmic microwave background radiation

Sergey G. Fedosin
PO box 614088, Sviazeva str. 22-79, Perm, Perm Krai, Russia
ORCID 0000-0003-3627-2369, E-mail: sergey.fedosin@gmail.com

The alternative mechanism of the emergence of cosmic microwave background radiation (CMB), associated with the thermal radiation of primordial gas-dust clouds in the early Universe, is considered. The emergence of such clouds in the theory of infinite hierarchical nesting of matter is a natural stage in matter evolution. The mass, radius, and spatial concentration of typical primordial gas-dust clouds, the distance between neighboring clouds, and the power of CMB energy generation per unit volume and per nucleon of the early Universe were calculated. The masses and radii of these clouds correspond to the masses and radii of the observed Bok globules. The presented mechanism is consistent with the cluster model describing the appearance of angular multipoles in the CMB power spectrum. In addition to CMB radiation, cosmic infrared background (CIB) radiation and cosmic optical background (COB) radiation are also considered. According to the presented model, the sources of CIB are primordial protoplanetary clouds. As for the COB radiation, it is associated with the radiation of the first protostars. During evolution, each primordial cloud, with a mass of about 31 solar masses, first generates CMB radiation, and then CIB and COB radiations. Since protostars give rise to neutron stars, the concentration of primordial gas-dust clouds is also the concentration of observed neutron stars. In the course of the calculations, a new definition of the radiation intensity is used, which is based on the vector of the surface energy flux density and accounts for the angles of incidence of radiation on a flat receiver from all sides of the hemisphere. According to Poynting's theorem, the relationship between the intensity and energy density of black body radiation is derived from the concept of photons.

Keywords: cosmic microwave background; infinite hierarchical nesting of matter; early Universe; cosmology: theory; matter evolution.

PACS: 98.70.Vc

1. Introduction

The cosmic microwave background radiation (CMB) in the wavelength range of 0.3-30 mm contributes most to the total energy of cosmic background radiation. The standard explanation for the origin of CMB based on the Big Bang concept, in which CMB appeared in the early Universe. However, the idea of the Big Bang still has drawbacks [1]; therefore, other alternative cosmological theories continue to appear. For example, in the quasi-steady-state cosmological model, it is assumed that CMB could be the result of processing stellar radiation by cosmic dust [2].

However, even in this case, there are difficulties associated with the fact that the CMB is too homogeneous and isotropic and has a spectrum of ideal black body. According to the dynamic Universe model [3] and the hierarchical Universe model [4], the stellar radiation in the early Universe could be sufficient for CMB to have the observed energy density and be isotropic, so that the Big Bang is not needed. According to [5], the models based on a Universe in dynamical equilibrium without expansion predicted the 2.7 K temperature prior to and better than models based on the Big Bang. In addition, it was shown in [6] that isotopes of all the observed chemical elements can be formed from hydrogen in stars during the time of the order of 100 billion years, which makes it possible to do without the Big Bang.

It is known from measurements [7] that the CMB temperature corresponds to the blackbody temperature $T = 2.7255$ K. If the CMB is in equilibrium with respect to some global blackbody of the Universe, it would have a volumetric energy density equal to $u = \frac{4\sigma T^4}{c} = 4.17 \times 10^{-14}$ J/m^3, where σ is the Stefan–Boltzmann constant, and c is the speed of light. This relation characterizes, for example, the state of a hollow black body, which is in thermal equilibrium with radiation in the inner cavity. The surface of such a cavity emits and absorbs radiation energy with an intensity of $I = \sigma T^4 = 3.13 \times 10^{-6}$ W/m^2. This means that ideal receivers, close in their properties to a blackbody, will measure in the cavity the CMB intensity on the order of I. In this case, the contribution to the intensity I will be made by photons incident on the receiver at various angles.

In measurements, the angular intensity $J = \frac{dI}{d\Omega}$ is often used, where Ω denotes the solid angle in steradians, from which the radiation arrives at the receiver. In accordance with the Stefan–Boltzmann law, for CMB radiation, if it were in thermal equilibrium with matter as in a hollow black body, the following relation would be true: $J = \frac{I}{\pi} = \frac{\sigma T^4}{\pi} = 9.96 \times 10^{-7}$ W/(sr·m^2). This value is in accordance with the results in [8].

When plotting the radiation spectrum of a blackbody, the dependence of the spectral angular intensity $\frac{dJ}{d\nu}$ on the radiation frequency ν is usually plotted. This value reaches a maximum when a small frequency range $d\nu$ is selected near the frequency $\nu_m = 160.23$ GHz, corresponding to the maximum in CMB radiation. In accordance with Wien's law of displacement for the frequency there is $\nu_m = \frac{\alpha}{h} kT \approx 5.879 \times 10^{10} \cdot T$, where the constant $\alpha \approx 2.821439...$, h is the Planck constant, k is the Boltzmann constant, and the radiation temperature T is measured in Kelvin.

The purpose of this work is to explain the origin of background radiation in the model of a hierarchical Universe. Based on the thermal equilibrium of radiation and matter of radiation sources in the early Universe, we will find the sizes of these sources, their masses and concentration in space. As will be shown below, in the presented approach the formula $u = \frac{4\sigma T^4}{c}$ for the energy density of background microwave radiation in the Universe can no longer be valid, as well as for background infrared radiation and background optical radiation.

2. Definition of intensity

The standard definition considers intensity as the amount of energy passing per unit of time through a unit area oriented perpendicular to the direction of energy propagation. To take into account various orientation angles of the receiver with respect to the incident radiation, a different definition should be applied. In the concept of photons, we can assume that intensity is the magnitude of a certain vector, namely the vector of the surface density of the radiation energy flux.

Let us assume that the radiation receiver responds only to the radiation component, which is perpendicular to the receiver plane. This can happen, for example, when the receiver is sensitive to the momenta of the photons falling on the receiver from all sides. Then the momenta components of the set of photons, which are parallel to the receiver plane, mutually cancel each other, and the sum of the perpendicular momenta components of the photons is considered. In this case, we can assume that the energy flux surface density vector **I** is determined by the amount of incident radiation energy on the flat radiation receiver from all sides of the hemisphere per second per unit area S of the receiver, taking into account the angular dependence:

$$\mathbf{I} = \sum_i \frac{d}{dS}\left[\frac{d\left(E_i \hat{\mathbf{p}}_i \cdot \hat{\mathbf{n}}\right)}{dt}\right]\hat{\mathbf{n}} = c\sum_i \frac{d}{dS}\left[\frac{d\left(\mathbf{p}_i \cdot \hat{\mathbf{n}}\right)}{dt}\right]\hat{\mathbf{n}} = \\ = c\sum_i \frac{d}{dS}\left(\mathbf{F}_i \cdot \hat{\mathbf{n}}\right)\hat{\mathbf{n}} = c\sum_i \frac{dF_{in}}{dS}\hat{\mathbf{n}} = c\sum_i P_{in}\,\hat{\mathbf{n}} = cP_n\,\hat{\mathbf{n}}. \tag{1}$$

where $E_i = c\,p_i$ denotes the energy of the photon with momentum amplitude p_i; the index i specifies the photon number during summation in (1); $\hat{\mathbf{p}}_i$ is a unit vector directed along the photon momentum $\mathbf{p}_i$, such that $\mathbf{p}_i = p_i\,\hat{\mathbf{p}}_i$; $\hat{\mathbf{n}}$ is a unit normal vector directed to the receiver plane from the hemisphere; $\mathbf{F}_i = \frac{d\mathbf{p}_i}{dt}$ defines the force acting from the photon on the receiver; $F_{in} = \left(\mathbf{F}_i \cdot \hat{\mathbf{n}}\right)$ is the force projection on the normal; $P_{in} = \frac{dF_{in}}{dS}$ denotes the pressure from the photon's side, perpendicular to the receiver surface; and $P_n = \sum_i P_{in}$ is the total perpendicular pressure from all photons.

If we take into account that the electromagnetic radiation pressure is $P = \frac{u}{3} = \frac{4I}{3c}$, then according to (1), we have

$$P_n = \frac{3P}{4}, \qquad \mathbf{I} = cP_n\,\hat{\mathbf{n}} = \frac{3cP}{4}\hat{\mathbf{n}}. \tag{2}$$

In (2), the vector $\mathbf{I}$ is directed in the same way as the unit normal vector $\hat{\mathbf{n}}$ and is proportional to the speed of light and the electromagnetic pressure on the receiver.

The difference between P_n and P in (2) can be attributed to the well-known 4/3 problem, according to which the mass-energy m_P of the electromagnetic field of a charged body moving at a very low velocity, derived from the Poynting vector and proportional to the field momentum density, is 4/3 times greater than the mass-energy m_E, corresponding to the field energy density. The relation $m_E = \frac{3m_P}{4}$ corresponds to the equality $P_n = \frac{3P}{4}$, so that the radiation pressure P is related to the Poynting vector, and the pressure P_n exerted on the receiver is related to the field energy density. According to [9], the 4/3 problem occurs because

the electromagnetic field energy density and the field momentum density are not the four-momentum components but rather the field stress-energy tensor components.

To check formula (1), first place the receiver on the surface of the sphere of radius r, at the center of which there is a certain source with the power of isotropic radiation W. In this situation, the radiation falls on the receiver at a right angle. In (1) the scalar product $\left(\hat{\mathbf{p}}_i \cdot \hat{\mathbf{n}}\right) = 1$ is obtained, and the energy flux density recorded in the receiver is then equal to:

$$I = \frac{W}{4\pi r^2}. \tag{3}$$

Let us consider another situation, when one of the many existing radiation sources is the volume element dV. We can assume that $dW = \frac{u\,dV}{\Delta t}$ is the differential of the radiation energy, leaving the volume element dV per unit time Δt. Let us choose the hemisphere radius $R = c\Delta t$, where c is the speed of light, and place the receiver at the coordinate origin on the plane ZOX at the center of the hemisphere. This situation is shown in Figure 1.

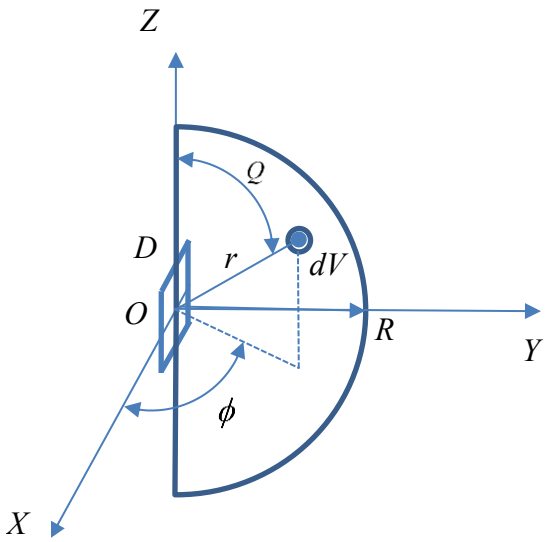

Fig. 1. The receiver D (in this case rectangular in shape) is located at the coordinate origin on the plane ZOX at the center of the hemisphere of radius R, the current radius r and the angles Q and ϕ specify the position of the radiating volume element dV in the spherical coordinate

Now, all the radiation energy contained in the hemisphere with a radius R falls into the receiver at time Δt. Then, in spherical coordinates for the intensity differential of the volume element dV located inside the hemisphere at a distance r from the center, in accordance with (1) and (3), we have:

$$dI = \frac{u \sin Q \ \sin\phi \ dV}{4\pi r^2 \Delta t}, \tag{4}$$

where $dV = r^2 dr \sin Q dQ \, d\phi$ is the volume element considered as a source of isotropic radiation; the product $\sin Q \ \sin\phi$ defines the angular dependence of the radiation intensity so that at $Q = 0$ photons move along the OZ axis and do not enter the receiver at all; and at $\phi = 0$, photons move in the ZOX plane and do not enter the receiver either. If $Q = \pi/2$, and $\phi = \pi/2$, photons fall on the receiver at a right angle to its surface and make the maximum contribution to the intensity. The appearance of $\sin Q \ \sin\phi$ in (4) follows from the fact that, according to Figure 1, $\hat{\mathbf{n}} = -(0,1,0)$, $\hat{\mathbf{p}}_i = -(\sin Q \ \cos\phi, \sin Q \ \sin\phi, \cos Q)$, and in definition (1), we have $(\hat{\mathbf{p}}_i \cdot \hat{\mathbf{n}}) = \sin Q \ \sin\phi$.

Integration over the hemisphere's volume replaces the summation in (1) and gives the following:

$$I = \frac{u}{4\pi\Delta t} \int_0^{R=c\Delta t} dr \int_0^{\pi} \sin^2 Q \ dQ \int_0^{\pi} \sin\phi \ d\phi = \frac{uc}{4}. \tag{5}$$

The calculation in (5) shows how, in the case of equilibrium blackbody radiation, we can understand the relation between the intensity I and the energy density u of radiation that enters the receiver from different directions. Hence, we can see that I is actually related to the mass-energy of the field energy density, and not to the mass-energy of the momentum density, which is found using the Poynting vector.

3. CMB energy production

It is known that CMB radiation originates from large distances; therefore, in one way or another, it is generated by many sources. Let us assume that, on average, each cubic meter of the early Universe was a source of CMB and produced L joules of CMB energy per second; then, the volumetric power L of energy generation is measured in W/m^3. Next, we proceed as in [4].

Let us suppose that radiation sources uniformly fill the hemisphere, while radiation from some sources does not fall on the receiver at a right angle. This means that to determine the intensity I, we should integrate the entire hemisphere's volume and take into account the angles of incidence of radiation on the receiver, similar to (4) and the definition of intensity in (1). We will place the receiver at the origin of the coordinate system and position it in the *ZOX* plane to measure the CMB energy.

If some radiating volume is located at a distance r from the origin of coordinates, then the effective amount of energy dI, incident per unit time on the unit area of the receiver, will be equal to:

$$dI = \frac{L\exp\left(-\frac{Hr}{c}\right)\exp\left(-snr\right)\sin Q\ \sin\phi\ dV}{4\pi r^2}, \tag{6}$$

where H is the Hubble constant.

The first exponent $\exp\left(-\frac{Hr}{c}\right)$ in (6) describes the exponential decrease in the energy of CMB photons as they travel a distance r. As a result, the wavelength of the photons is shifted, which is known as the cosmological redshift of the spectra of distant radiation sources.

The second exponent $\exp(-snr)$ sets the degree of scattering of photons on their way to the receiver, reducing the number of arriving photons. This exponent corresponds to the Beer–Lambert law for light scattering, and s is the scattering cross section, n is the concentration of objects scattering light.

Let us take the integral in (6) over the volume of the hemisphere of infinite radius:

$$I = \frac{L}{4\pi}\int_0^{\infty}\exp\left(-\frac{Hr}{c}\right)\exp(-snr)\,dr\int_0^{\pi}\sin^2 Q\;dQ\int_0^{\pi}\sin\phi\;d\phi = \frac{L}{4\left(\frac{H}{c}+sn\right)}. \qquad (7)$$

In (7), the relation between the measured intensity I and the volumetric power L of CMB energy generation in cosmic space is presented.

Considering that the exponent $\exp\left(-\frac{Hr}{c}\right)$ in (7) describes the exponential decrease in energy, as well as in the frequency of CMB photons as they travel a distance r, the following is obtained for the photon wavelength and redshift:

$$\lambda = \lambda_0\exp\left(\frac{Hr}{c}\right), \qquad z = \frac{\lambda-\lambda_0}{\lambda_0} = \frac{\lambda}{\lambda_0}-1 = \exp\left(\frac{Hr}{c}\right)-1, \qquad r = \frac{c}{H}\ln(z+1). \qquad (8)$$

If in (8) z is small compared to unity, then $\ln(z+1)\approx z$, which leads to the Hubble law in the form $r \approx \frac{cz}{H}$.

Due to the decrease in energy and scattering of photons in (6), some blurring of images of distant galaxies should be observed, since photons change their motion direction as a result of scattering. In fact, the observed blurring is insignificant, which can be explained by the small size of the electrogravitational vacuum particles described in [4] and [10], which are unable to significantly change the direction of the photons' momenta. We can also refer to more recent works [11-12], in which, in light of new data, the observed dependence of the duration of supernova explosions on the distance to them, the dependence of the surface brightness of galaxies on the redshift, the relationship between redshift, relict radiation, and the blackbody spectrum were analyzed.

In addition, observations of the angular radii and surface brightness of galaxies at a given luminosity do not correspond to the expanding Universe hypothesis in the $\Lambda - CDM$ model, but are in good agreement with relation (8), which describes the relationship between distance and redshift, as well as with the static Universe model [13-14], in which the surface brightness does not depend on the redshift z. With relation (8), the supernovae type Ia data give almost the same result as the $\Lambda - CDM$ model.

4. The sources of CMB

In the theory of infinite hierarchical nesting of matter [4], [10], [15], it is assumed that the substance of a certain level of matter arises in the course of evolution of the substance of lower levels of matter. Therefore, stars as objects of the stellar level of matter appear after the compression of large gas clouds. The main objects of these clouds are nucleons belonging to the nucleon level of matter. In turn, the appearance of gas clouds is a consequence of evolution of the substance of the praon level of matter, and praons can form the substance of nucleons in the same way as nucleons can form the substance of stars.

Based on this, suppose that in the early Universe, the entire volume was more or less uniformly filled with CMB sources at concentration n, the average radius of these sources was equal to a, and the effective temperature of particles on the surface of these sources was equal to the temperature T_s. In this case, we can write:

$$L = 4\pi\sigma T_s^4 a^2 n. \tag{9}$$

In (9), the CMB generation power per unit volume L is expressed through the surface area of a typical CMB source, equal to $4\pi a^2$, through the intensity σT_s^4 of radiation from this surface, and through the concentration n of CMB sources in Universe.

Substituting L from (7) in (9) and taking into account that $I = \sigma T^4$, we find:

$$\frac{T_s^4 a^2 n}{\left(\frac{H}{c} + sn\right)} = \frac{T^4}{\pi}. \tag{10}$$

We assume that during the time needed for CMB photons to reach the Earth from distant regions of the Universe, the number of baryons and their concentration in cosmic space did not change significantly. Then, in the first approximation, we can use the conclusions of the $\Lambda - CDM$ model (Lambda-cold dark matter model), where the critical mass density reaches the value $\rho_{cr} = \frac{3H^2}{8\pi G} = 9.2 \times 10^{-27}$ kg/m^3, if we assume that the Hubble constant H equals 70 km/(s·Mpc) or 2.268×10^{-18} s^{-1} [16].

The physical density of the visible baryonic matter in this case is $\rho_b = 0.0227 \rho_{cr} = 2.1 \times 10^{-28}$ kg/m^3. This value is chosen in such a way that, among other things, it best fits observations of the amount of visible matter in galaxies. This approach will be sufficient for us since we will further derive various relationships, the physical meaning of which does not depend on the specific value of ρ_b.

Let us now take into account that the CMB sources, that is, the primordial gas-dust clouds, were located discretely in space with a concentration $n = \frac{\rho_b}{m}$, where m is the mass of a typical CMB source. Each source has a cross section equal to $s = \pi a^2$. At very large distances, all sources begin to overlap each other, which makes it difficult to see the most distant CMB sources and weakens the intensity of the radiation that could be at the radiation receiver. This leads to the appearance of the exponent $\exp(-snr)$ in (6).

The mass of a typical source is expressed by the formula $m = \frac{4\pi a^3 \rho_s}{3} = \frac{\rho_b}{n}$, where ρ_s is the mass density of the source substance. Expressing n from here and substituting into (10), taking into account the equality $s = \pi a^2$, we have:

$$n = \frac{\rho_b}{m} = \frac{3\rho_b}{4\pi a^3 \rho_s}, \qquad \frac{T_s^4}{\left(1 + \frac{4Ha\rho_s}{3c\rho_b}\right)} = T^4 . \tag{11}$$

The last formula in (11) relates the radius a, mass density ρ_s of CMB sources and the effective temperature T_s of the surface particles of these sources.

5. The origin of energy in CMB sources

For the particles of numerous CMB sources to have a kinetic temperature on the order of T_s and to be able to subsequently radiate at this temperature, it is necessary that the particles of these sources somehow acquire the corresponding thermal energy as the energy of proper motion.

Let us turn to the theory of infinite hierarchical nesting of matter, according to which different matter levels are found in the Universe, and the main objects of these levels have significantly different masses and sizes. In particular, there are metagalactic, stellar, nucleon, praon, and graon levels of matter [4], [10], [15], [17-21].

All matter levels structured by gravitational clustering. This process is accompanied by the opposite process of fragmentation when particles collide with each other and with radiation quanta. In large gas clouds, under appropriate conditions, atoms and molecules can combine under the action of gravitational forces first into molecular complexes and then into more massive dust particles, until planets, stars and their clusters are formed. Dust particles of micron size have a fairly dense core surrounded by a layer of loose matter. The minimum time required for the formation of such particles can be estimated by the approximate formula for the radial fall of matter to the accretion center under the action of gravitation [22]:

$$t \approx \sqrt{\frac{3}{2\pi G\rho}}, \tag{12}$$

where G is the gravitational constant, and ρ is the mass density of matter at the initial moment of fall. For example, with a density of $\rho = 100$ kg/m^3 in (12) we obtain a duration of approximately 2.3 hours. The lower the initial mass density of an object is, the longer it takes for such an object to be formed. For a gas cloud with an initial density of $\rho = 10^{-20}$ kg/m^3, the time t will be approximately 2.7×10^7 years. If we substitute in (12) the current density of baryonic matter $\rho = \rho_b = 2.1\times10^{-28}$ kg/m^3, the corresponding duration of metagalaxy formation will be on the order of 180 billion years.

A more accurate calculation accepted in astrophysics takes into account the time required for a gas cloud to increase its density with decreasing radius instead of taking into account the time of fall into the accretion center. Let us assume that the evolution of matter in the hierarchically structured Universe leads over time to the formation of baryonic matter with average mass density ρ_b. This process cannot be uniform everywhere, and in those places,

where it goes faster, the matter can compress under the action of gravitation, regardless of the surrounding volumes of space with lower density. For acceleration the particles' motion in the gravitational field outside the gas cloud with the mass M, we have:

$$\frac{d^2r}{dt^2} = -\frac{GM}{r^2}. \tag{13}$$

This equation (13) is also suitable for describing the motion of the gas cloud's outer shell. The solution of (13) should be sought in the form $\frac{dr}{dt} = \pm\sqrt{\frac{A}{r} + B}$, $\frac{d^2r}{dt^2} = -\frac{A}{2r^2}$.

Hence, it follows that $A = 2GM$, and if $B = -\frac{2GM}{r_b}$, where r_b is the initial radius of the cloud, we obtain the relation for the velocity of the shell motion, which is associated with the law of conservation of energy:

$$\left(\frac{dr}{dt}\right)^2 = \frac{2GM}{r} - \frac{2GM}{r_b}. \tag{14}$$

For the case of cloud compression, the coordinate r decreases over time t, and therefore, we use the following equation:

$$\frac{dr}{dt} = -\sqrt{\frac{2GM}{r} - \frac{2GM}{r_b}}. \tag{15}$$

The solution of the differential equation (15), in the case of compression from radius r_b to radius r_s, is as follows:

$$t = \left[\frac{\sqrt{r_b}\,r}{\sqrt{2GM}}\sqrt{\frac{r_b}{r} - 1} + \sqrt{\frac{r_b^3}{2GM}}\,\mathrm{arctg}\sqrt{\frac{r_b}{r} - 1}\right]\Bigg|_{r_b}^{r_s} = \frac{\sqrt{r_b}\,r_s}{\sqrt{2GM}}\sqrt{\frac{r_b}{r_s} - 1} + \sqrt{\frac{r_b^3}{2GM}}\,\mathrm{arctg}\sqrt{\frac{r_b}{r_s} - 1}. \tag{16}$$

The maximum time is reached when the matter falls onto the point center with the radius $r_s = 0$. Assuming that $r_b = \left(\frac{3M}{4\pi\rho_b} \right)^{1/3}$, in the case in (16), $t_{\max} = \frac{\pi}{2}\sqrt{\frac{r_b^3}{2GM}} = \sqrt{\frac{3\pi}{32G\rho_b}}$. This time depends only on the initial mass density ρ_b of the cloud and is estimated, since the solution does not consider the pressure forces in the gas cloud, which rapidly increase as the radius decreases.

Considering this approach, two scenarios are possible. In the first of them, the matter of the observable Universe with an average density ρ_b arises from praons, the smallest particles of the lowest level of matter, in a period of time determined by the physical conditions of this process. To understand how a nucleon can be formed from a set of praons, it is enough to imagine a similar process, in which a set of nucleons in a large gas cloud is compressed to the maximum extent under the action of gravitation. If the mass of the emerging star is large enough, then the result of its evolution would be a supernova and the birth of a neutron star. Praons, nucleons and neutron stars are similar because they have the highest possible mass densities and the strongest electromagnetic fields at their levels of matter. In this case, it is assumed that at the level of nucleons the particles' matter is held together not by ordinary gravitation but by strong gravitation [10], [15].

In the second case, baryonic matter is first created; this matter is distributed in space with a certain mass density ρ_m and subsequently compressed to density ρ_b. Let ρ_b significantly exceed ρ_m. By substituting $r_b = \left(\frac{3M}{4\pi\rho_b} \right)^{1/3}$ instead of r_s and $r_m = \left(\frac{3M}{4\pi\rho_m} \right)^{1/3}$ instead of r_b, and neglecting the first term in (16), we obtain $t_{\text{m}} \approx \sqrt{\frac{3\pi}{32G\rho_m}}$. As an estimate, we will substitute here $\rho_b = 2.1\times10^{-28}$ kg/m^3 instead of ρ_m and will obtain the corresponding minimum compression time, if it actually took place: $t_{\min} \approx \sqrt{\frac{3\pi}{32G\rho_b}} = 145$ billion years.

For comparison, in the standard cosmological $\Lambda - CDM$ model, based on the general theory of relativity, the age of the Metagalaxy is estimated to be approximately 13.8 billion years. Moreover, in order to explain the spatial flatness, homogeneity, isotropy and large-scale structure of Metagalaxy, the model includes the hypothesis of cosmological inflation at the early stages of the Big Bang. The exotic character of such inflation is associated with the fact that during a period of time from 10^{-42} sec to 10^{-36} sec after the start of the Big Bang at the

initial Planck matter density of approximately 10^{96} kg/m^3 the radius of the Metagalaxy should have increased by a factor of 10^{26} [23]. As can be seen from the estimates made above, if the hypothesis of cosmological inflation is not used, the minimum age of the observable Universe should be an order of magnitude greater than in the $\Lambda - CDM$ model.

We can consider a typical CMB source as a relativistic uniform system and estimate its internal thermal energy using the virial theorem [24-25]. Considering the contributions of gravitational energy and pressure field energy to the system's potential energy, according to [26], the following relation is obtained for the kinetic energy E_k:

$$E_k \approx \frac{81Gm^2}{100\sqrt{14}a}. \tag{17}$$

However, the energy E_k can be approximately expressed in terms of the average temperature T_s of the source:

$$E_k \approx \frac{3mkT_s}{2m_p}, \tag{18}$$

where the ratio of the source mass to the nucleon mass in the form $\frac{m}{m_p} = N$ specifies the total number of nucleons N as an estimate of the total number of atoms, and k is the Boltzmann constant.

Comparing expressions (17) and (18) for E_k in view of the relation $m = \frac{4\pi a^3 \rho_s}{3}$ gives us the following:

$$a = \sqrt{\frac{25\sqrt{14}kT_s}{18\pi G m_p \rho_s}}. \tag{19}$$

A primordial gas-dust cloud with mass m, which is the source of CMB, can be considered as a blackbody, in which matter is in thermal equilibrium with CMB radiation. The radiation

energy density inside the cloud should be equal to $u_s = \frac{4\sigma T_s^4}{c}$. When a typical CMB source is formed in the form of a gas-dust cloud, the binding energy ΔE should be released, which is equal in order of magnitude to the total kinetic energy E_k of the cloud particles. A more precise estimate in [26] gives $\Delta E \approx \frac{5}{3}\left(\frac{14\sqrt{14}}{27} - 1\right) E_k \approx 1.57 E_k$. We can assume that the binding energy ΔE is radiated from the cloud by means of CMB radiation. In this case, the following equality must be satisfied:

$$u_s = \frac{4\sigma T_s^4}{c} = \frac{\Delta E}{V_s} = \frac{4.71 E_k}{4\pi a^3}, \tag{20}$$

where $V_s = \frac{4\pi a^3}{3}$ is the cloud's volume.

Substituting E_k from (18) in (20) and considering the relation $m = \rho_s V_s$, we find:

$$\rho_s = \frac{8\sigma T_s^3 m_p}{4.71 ck}. \tag{21}$$

6. Parameters of CMB sources

Relations (11), (19) and (21) can be considered as a system of three equations to determine unknown quantities a, T_s and ρ_s. Substituting ρ_s (21) into (19), we get:

$$a = \frac{5k}{12 T_s m_p}\sqrt{\frac{4.71\sqrt{14}\, c}{\pi G \sigma}}. \tag{22}$$

Multiplying a (22) by ρ_s (21), we find:

$$a\rho_s = \frac{10 T_s^2}{3}\sqrt{\frac{\sqrt{14}\,\sigma}{4.71\,\pi c G}}. \tag{23}$$

Substituting (23) into (11) leads to a quadratic equation for T_s^2:

$$T_s^4 - T_s^2 \frac{40HT^4}{9\rho_b}\sqrt{\frac{\sqrt{14}\,\sigma}{4.71\pi c^3 G}} - T^4 = 0\,. \tag{24}$$

Solving equation (24) gives the surface temperature of a typical CMB source:

$$T_s = T\sqrt{\frac{20HT^2}{9\rho_b}\sqrt{\frac{\sqrt{14}\,\sigma}{4.71\pi c^3 G}} + \sqrt{\frac{400\sqrt{14}\,H^2T^4\sigma}{81(4.71)\pi c^3 G\rho_b^2}} + 1} = 3.472 \text{ K.} \tag{25}$$

Substituting T_s (25) into (22) and into (21), we obtain the radius a of the CMB source in the form of a gas-dust cloud and the density ρ_s of the substance of the cloud:

$$a = 2.088\times10^{16} \text{ m.} \qquad \rho_s = 1.629\times10^{-18} \text{ kg/m}^3. \tag{26}$$

The radius of the cloud in (26) reaches the value $a = 0.68$ pc.

Next, taking into account (26), we find the mass of the source:

$$m = \frac{4\pi a^3 \rho_s}{3} = 6.21\times10^{31} \text{ kg or } 31.2\,M_c\,, \tag{27}$$

where M_c is the mass of the Sun.

Parameters (26-27) of a typical CMB source correspond to a rather large gas-dust cloud, the particles of which acquire their kinetic energy due to gravitational work to compress matter. When the particles collide, the energy of motion is converted into heat and can then be radiated in the form of CMB quanta.

If we take into account that the obtained in (26-27) parameters of the sources belong to gas clouds in the early Universe, then we can expect that the first stars appeared precisely in such clouds. Later, similar clouds could give rise to the first open star clusters, which became the main elements of emerging galaxies. For comparison, the number of stars in currently observed open star clusters can be more than one hundred, the typical masses of clusters can exceed

$50M_c$, the core's radius can reach approximately 0.6 pc, and the radius of the corona in a typical cluster can reach 6 pc.

The concentration of CMB sources in the early Universe is found through the density of baryonic matter ρ_b and the mass m of a typical source according to the first relation in (11):

$$n = \frac{\rho_b}{m} = 3.4 \times 10^{-60} \text{ m}^{-3}. \tag{28}$$

If we assume that each source is located in a certain cubic volume in a cubic lattice, then the shortest distance between the nearest sources will equal $R_s = \frac{1}{\sqrt[3]{n}} \approx 6.7 \times 10^{19}$ m. This means that the distance between the centers of the nearest sources is $\frac{R_s}{a} \approx 3.2 \times 10^3$ times greater than the radius a of a typical source and is equal to the value on the order of $R_s \approx 2.16$ kpc at $a = 0.68$ pc according to (26).

The value of L, that is CMB generation power per unit volume of the Universe, is found from (9) taking into account T_s (25), a (26) and n (28), or from (7) taking into account the relations $I = \sigma T^4$, $s = \pi a^2$:

$$L = 4\pi\sigma T_s^4 a^2 n = 4\sigma T^4 \left(\frac{H}{c} + \pi a^2 n \right) = 1.53 \times 10^{-31} \text{ W/m}^3. \tag{29}$$

The values of L may differ slightly in different directions, reflecting the variability of the Hubble parameter and the spatial matter distribution.

The average concentration of nucleons in the Universe is $n_b = \frac{\rho_b}{m_p} = 0.125$ m^{-3}. Taking this into account, from (29) the power of CMB energy generation per nucleon of the Universe is determined:

$$\frac{L}{n_b} = 1.22 \times 10^{-30} \text{ W/ nucleon}. \tag{30}$$

Dividing the binding energy $\Delta E \approx 1.57 E_k$ of one SMB source by the number $N = \frac{m}{m_p}$ of nucleons in this source, taking into account expressions E_k (18) and T_s (25), we find the binding energy per nucleon:

$$\frac{\Delta E}{N} = \frac{4.71\, k T_s}{2} = 1.1 \times 10^{-22} \text{ J/ nucleon.} \tag{31}$$

On the other hand, an estimate of the photon's concentration in the volume of a CMB source in a state of temperature equilibrium between radiation and matter at the temperature $T_s = 3.472$ K is obtained as $n_f = \frac{\beta\, s_f}{k} = 8.49 \times 10^8$ m^{-3}, where

$$s_f = \frac{16 \sigma T_s^3}{3c} = \frac{4 u_s}{3 T_s} = 4.22 \times 10^{-14} \text{ J/(K·m}^3\text{)}$$

is the volumetric density of the CMB entropy and the coefficient $\beta = \frac{45}{4\pi^4} \int_0^\infty \frac{\xi^2 d\xi}{e^\xi - 1} \approx 0.2776...$

Dividing the photon energy density $u_s = \frac{4 \sigma T_s^4}{c}$ (20) by the photon concentration n_f, we obtain the average energy per photon:

$$\frac{u_s}{n_f} = \frac{3kT_s}{4\beta} = 1.29 \times 10^{-22} \text{ J/photon.} \tag{32}$$

Note that the binding energy per nucleon $\frac{\Delta E}{N}$ in (31) and the energy per photon $\frac{u_s}{n_f}$ in (32) are close to each other in magnitude. After the photons leave the CMB sources, fill outer space and reach the Earth, their average temperature will decrease from value $T_s = 3.472$ K to value $T = 2.7255$ K. In this case, the energy of a photon with a frequency of $\nu_m = 160.23$ GHz corresponding to the maximum in CMB radiation at temperature $T = 2.7255$ K is equal to $h\nu_m = 1.06 \times 10^{-22}$ J.

Hence, the ratio of the number of CMB photons in cosmic space to the number of matter nucleons present in this space should be on the order of unity. On average, we can assume that each nucleon of the observable Universe produces only one CMB photon.

In the course of our calculations, we assumed that all the nucleons present in the Universe with an average density of $\rho_b = 2.1\times10^{-28}$ kg/m^3 were compressed by gravitation into primordial gas-dust clouds with an average density of $\rho_s = 1.629\times10^{-18}$ kg/m^3 (26). These clouds play the role of typical CMB sources. Let the volume of a typical source be denoted by $V_s = \frac{m}{\rho_s} = \frac{4\pi a^3}{3}$ and the volume of the same, but not compressed matter in the homogeneous Universe with density ρ_b and with the same mass m (27) be denoted by V. Then, the ratio of the volumes equals $\frac{V}{V_s} = \frac{\rho_s}{\rho_b} = 7,76\times10^9$. Now, in view of E_k (18), the binding energy $\Delta E \approx 1.57E_k$ of one source, and the number of nucleons $N = \frac{m}{m_p}$ in the source, we can estimate the average CMB energy density in the Universe in the following form:

$$\bar{u} = \frac{\Delta E}{V} = \frac{1.57E_k\rho_b}{V_s\rho_s} = \frac{1.57E_k\rho_b}{m} = \frac{1.57\rho_b}{m}\frac{3kT_sN}{2} = \frac{4.71\rho_bkT_s}{2m_p} = 1.4\times10^{-23}\ \text{J/m}^3. \quad (33)$$

When deriving relation (20), we use the expression $u_s = \frac{\Delta E}{V_s}$. Combined with (33) and the relation $\frac{V}{V_s} = \frac{\rho_s}{\rho_b} = 7.76\times10^9$, this gives the following:

$$\frac{u_s}{\bar{u}} = \frac{V}{V_s} = \frac{\rho_s}{\rho_b} = 7.76\times10^9. \quad (34)$$

In (34), a significant difference is obtained between the averaged CMB energy density $\bar{u}$ in (33), and between the photon energy density u_s in the case of thermal equilibrium of photons with the matter of CMB sources. The difference in magnitudes of u_s and $\bar{u}$ results from the fact that the CMB generated in the volume V_s of each source was in equilibrium with the matter only in this volume. When the CMB from each source fills the volume V and starts mixing

with the radiation from nearby sources, the CMB energy density decreases from u_s to $\bar{u}$. As a result, the SMB observed on Earth is thermal radiation, the energy density of which in the Universe. is $\bar{u}$.

In $\Lambda - CDM$ model, the difference in quantities of u_s and $\bar{u}$ is not taken into account, and it is assumed that the energy density of the CMB is equal to $u = \frac{4\sigma T^4}{c} = 4.17 \times 10^{-14}$ J/m^3 in the entire space of the Universe at temperature $T = 2.7255$ K of CMB.

In this case, the estimate of the CMB photon concentration in the form $n_f = \frac{\beta s_f}{k} = \frac{16\beta\sigma T^3}{3ck} = \frac{4\beta u}{3kT} = 4.1 \times 10^8$ m^{-3} applies to the entire Universe. Then the ratio of the number of CMB photons to the number of nucleons will equal $\frac{n_f}{n_b} = \frac{n_f m_p}{\rho_b} = 3.3 \times 10^9$, which is close in magnitude to the ratio of the volumes $\frac{V}{V_s}$ in (34).

Hence, the following question arises: why is the number of photons so much greater than the number of nucleons? This problem, known in cosmology as the entropy problem, is usually solved via the concept of the hot Universe based on the assumption of adiabatic space expansion from the initial state of equilibrium of radiation and matter.

In contrast, in our approach the numbers of CMB photons and nucleons are approximately the same, and there is no need for the hot Universe. Since the SMB is currently not in equilibrium with matter, the formula for energy density $u = \frac{4\sigma T^4}{c}$ cannot be applied to the entire Universe. Indeed, the primordial gas-dust clouds, which were the sources of CMB in the early Universe, were located in a discrete way, occupied a small volume and therefore could not play the role of a global black body, limiting the volume of the Universe.

7. The angular harmonics of CMB

Using the Fourier transform, the observed CMB power spectrum can be expanded to include spherical harmonics [27-28].

The spherical harmonic $\ell = 0$ in the angular power spectrum corresponds to the average value of the CMB temperature. The dipole anisotropy on the CMB temperature distribution map has an amplitude of approximately 0.1% and is related to the spherical harmonic $\ell = 1$ [29]. The dipole anisotropy is well explained by the Doppler effect and by the motion of the

Earth together with the Sun relative to the reference frame, in which the CMB intensity is the same in all directions. This motion changes the CMB radiation wavelength measured on Earth, depending on the angle between the Earth's total velocity in cosmic space and the direction of the sky region from which the CMB originates.

The spherical harmonics $\ell \geq 2$ are related to CMB temperature fluctuations, the root-mean-square deviation of which reaches several tens of μK relative to the average temperature. The $\Lambda - CDM$ model assumes that such temperature fluctuations could be caused by fluctuations in the density of matter in the early Universe, which had the state of very dense hot plasma of electrons and baryons.

One alternative explanation is that the angular power spectrum of the CMB can be obtained if CMB photons, upon their appearance, interact with matter, which was structured into some objects, clusters and particles [30]. The average distance between the centers of the objects in the case of their cubic arrangement is approximately 108 m, the mass of one object is 8.8×10^{-17} kg, and the mass density of the object is 9×10^{-23} kg/m^3. Similarly, there are clusters inside the objects, the distance between the centers of which is about 12 cm. If their mass density is 9×10^{-23} kg/m^3, then the cluster mass is 1.2×10^{-25} kg. The position and amplitude of the main peak of CMB power spectrum at $\ell \approx 360$ and of the subsequent peaks depend mainly on the mutual distances between the mentioned objects, and on their mass density and internal structure.

It is assumed that the cluster contains 40 to 100 particles, such as protons, helium nuclei and electrons; therefore, it represents an atomic-molecular complex, containing hydrogen and helium. On average, an object contains approximately 10^9 clusters. The results obtained for the structure of objects, clusters and particles were found under the condition of using a radiation wavelength equal to 1.9 mm. This wavelength corresponds to the maximum blackbody spectrum distribution at the temperature $T = 2.7255$ K and most exactly reflects the properties of CMB from the standpoint of structural analysis. Moreover, the angular power spectrum of CMB radiation is the same for all wavelengths of the CMB.

The presented parameters can be combined with the described scheme of CMB emergence in the early Universe, in which matter evolution first leads to formation of nucleons and electrons. Then gravitation compresses the matter into gas-dust clouds and sets the matter particles in motion. When the particles collide, the kinetic energy is converted into thermal energy and is radiated in the form of CMB photons. The mass density of objects in [30] is less than the mass density of gas clouds $\rho_s = 1.629 \times 10^{-18}$ kg/m^3, as found in (26). We can assume

that the objects in [30] were located in the less dense part of the shell of gas clouds. Then, CMB photons, passing through these objects, clusters and particles inside them, can form the currently observed angular radiation power spectrum.

The possibility that these objects, clusters and particles could appear in primordial gas clouds follows from the value of the Jeans mass [31], which can be simplified as follows:

$$M_J \approx 26 M_c \left(\frac{T}{10}\right)^{3/2} \left(\frac{10^9}{n}\right)^{1/2}. \tag{35}$$

The temperature T in (35) must be specified in K, and the particle concentration n must be specified in m^{-3}.

Let us substitute in (35) the cloud surface temperature $T_s = 3.472$ K (25) instead of T, and take into account $\rho_s = 1.629 \times 10^{-18}$ kg/m^3 (26) and the concentration of cloud particles $n_s = \frac{\rho_s}{m_p} = 9.7 \times 10^8$ m^{-3} instead of n. This gives $M_J = 5.4 M_c$. The Jeans mass is less than the gas cloud mass $m = 31.2 M_c$ (27), which allows fragmentation of the cloud into smaller structural components.

The nonuniform distribution of matter in cosmic space also contributes to the small-scale fluctuations in the CMB temperature. Thus, correlations between the optical radiation of galaxies and CMB fluctuations are described in [32], and for radio sources, such correlations are presented in [33]. The cold anomalies in CMB temperature are mysterious and cannot be explained from the standpoint of the $\Lambda - CDM$ model, the most famous of which is the WMAP cold spot discovered by the WMAP space observatory in the Eridanus constellation [34-35]. The cold spot is approximately $dT = 73$ μK colder than the CMB temperature, $T = 2.7255$ K.

These anomalies can be explained as follows. Since $I = \sigma T^4$ for CMB, in the first approximation, we have $dI = 4\sigma T^3 dT$. If we direct the radiation receiver exactly to the anomalous spot, then in (6), we can set $Q = \frac{\pi}{2}$, $\phi = \frac{\pi}{2}$, and we can write the following:

$$dI = 4\sigma T^3 dT = \frac{L \exp\left(-\frac{Hr}{c}\right) \exp(-snr)\, dV}{4\pi r^2}. \tag{36}$$

According to (7) and considering the relation $I = \sigma T^4$, we find:

$$I = \sigma T^4 = \frac{L}{4\left(\frac{H}{c} + sn\right)}, \qquad L = 4\sigma T^4 \left(\frac{H}{c} + sn\right). \tag{37}$$

Substituting L (37) into the expression for dI (36), we find the relationship between the temperature difference dT, the distance r and the volume dV generating CMB radiation and leading to the contribution dT to the CMB temperature T:

$$dT = \frac{T\left(\frac{H}{c} + sn\right)\exp\left(-\frac{Hr}{c}\right)\exp\left(-snr\right)\, dV}{4\pi r^2}. \tag{38}$$

Equation (38) assumes that the volume dV contains primordial gas-dust clouds functioning as CMB sources, which, on average, have the mass density $\rho_s = 1.629 \times 10^{-18}$ kg/m^3 (26) and the concentration $n = \frac{\rho_b}{m} = 3.4 \times 10^{-60}$ m^{-3} (28) in the early Universe. In this case, the concentration n is present in (38) in two terms. An increase n in the term $\left(\frac{H}{c} + sn\right)$ leads to an increase of dT, but the term $\exp\left(-snr\right)$ acts in the opposite way, reducing dT. Thus, if in some direction in the volume dV the concentration of sources differs from the value n due to some anomaly, then this will lead to a change of dT in (38).

We can see from the relation $n = \frac{\rho_b}{m}$ that if the mass m of a typical CMB source is constant, then the change in the concentration of sources n can be associated with a local change in the mass density of baryons ρ_b in the volume dV under consideration. Thus, fluctuations in the mass density ρ_b in cosmic space can influence fluctuations in the measured CMB temperature in various directions.

According to (8), the redshift z in the model under consideration can be related to the distance r by the formula: $r = \frac{c}{H}\ln\left(z+1\right)$. As an example, let us place a certain volume dV

at a distance corresponding to $z = 2$, that is, at $r = \frac{c}{H} \ln 3 = 4.7$ Gpc. Let us assume that dT equal to 20 μK, which is close to the value of the root-mean-square small-scale CMB fluctuations. Using further the relation $s = \pi a^2$, the values of $a = 2.088 \times 10^{16}$ m (26) and $n = 3.4 \times 10^{-60}$ m^{-3} (28), from (38) we find $dV = 9.35 \times 10^{74}$ m^3, which for a spherical volume gives the radius of this volume of the order of $R_v = 197$ Mpc. Such the radius is close to the radius of the known Giant Void in the constellation Canes Venatici [36]. Consequently, the presence of voids in accordance with (38) leads to the observed CMB fluctuations.

It is known that, for sufficiently large spherical harmonics ℓ the relation $\theta = \frac{2\pi}{\ell}$ holds true, where θ is the effective sky viewing angle [28]. The main peak in the CMB angular power spectrum occurs at $\ell \approx 360$, which corresponds to the angle $\theta \approx 1°$. Moreover, if the harmonic number $\ell < 360$ and ℓ decreases, and the angle $\theta > 1°$ and θ increases, the power in the angular spectrum decreases gradually without any particular peaks. Why do harmonics with small ℓ manifest in the spectrum in a different way than harmonics with large $\ell > 360$, which form the spectrum in the form of sinusoid damping in amplitude?

For the above example with the volume dV, let us calculate the angle θ in radians using the formula: $\theta = \frac{2R_v}{r} = 0,084$, and the angle in degrees $\theta° = \frac{180\,\theta}{\pi} = 4°,8$. The angle θ in radians corresponds to the spherical harmonic $\ell = \frac{2\pi}{\theta} = 75$ in the CMB angular power spectrum. It turns out that supervoids with a low density of matter or, on the contrary, denser regions of space can make a significant contribution to CMB temperature fluctuations only at small ℓ. As for the appearance of spherical harmonics with large values $\ell > 360$ in the power spectrum, in the model presented above, according to [30], they are explained by the fact that CMB radiation interacts with matter, which is structured into some objects, clusters, and particles. Thus, different mechanisms lead to different forms of CMB power spectrum for small and large spherical harmonics. In contrast, the $\Lambda - CDM$ model has difficulties explaining the low power and form of the angular spectrum for harmonics associated with large angles θ and with small ℓ [37].

8. Infrared and optical background radiation

The dependence of the angular intensity J on the cosmic background radiation frequency in [9] shows that there are other angular intensity peaks near the CMB, including those of the

cosmic infrared background (CIB) and the cosmic optical background (COB). The total intensity of CIB and COB radiation is almost 10 times less than the intensity of cosmic microwave background radiation (CMB).

It is believed that the main contribution to CIB and COB comes from the processing of radiation from protostars and young stars by cosmic dust. We can make this assumption more concrete. Let us apply the obtained results with respect to the CMB to estimate the parameters of space objects, which could produce CIB and COB radiation.

We can assume that the maximum J for the CIB is obtained at a radiation frequency of $\nu_{CIB} \approx 2\times10^{12}$ Hz, and for the COB the maximum occurs at a frequency of $\nu_{COB} \approx 3\times10^{14}$ Hz. As a first approximation, let us assume that the Wien displacement law for radiation from a black body is valid for the radiation frequency. This gives the corresponding radiation temperatures $T_{CIB} = 34$ K and $T_{COB} = 5103$ K.

Substituting temperatures T_{CIB} and T_{COB} in (25) instead of temperature T makes it possible to estimate the surface temperatures of CIB and COB sources in the early Universe:

$$T_{s\,CIB} = 426 \text{ K.} \qquad T_{s\,COB} = 9.6\times10^{6} \text{ K.} \tag{39}$$

Substituting temperatures (39) into (21-22) instead of T_s, we obtain the corresponding mass densities and radii of CIB and COB sources. We can also estimate the masses of sources by multiplying the mass density and the volume of the corresponding source:

$$\rho_{s\,CIB} = 3.01\times10^{-12} \text{ kg/m}^3. \qquad a_{CIB} = 1.7\times10^{14} \text{ m.} \qquad m_{CIB} = 6.19\times10^{31} \text{ kg.} \tag{40}$$

$$\rho_{s\,COB} = 34 \text{ kg/m}^3. \qquad a_{COB} = 7.5\times10^{9} \text{ m.} \qquad m_{COB} = 6.008\times10^{31} \text{ kg.} \tag{41}$$

According to (40), the sources of CIB radiation are gas-dust clouds with a radius of the order of $a_{CIB} = 1136$ AU. and with mass $m_{CIB} = 31.1 M_c$. For comparison, in the Solar System the dwarf planet Sedna at aphelion moves away from the Sun at a distance of 937 AU. From (41) it follows that COB radiation sources are objects with mass $m_{COB} = 30.2 M_c$ and with a radius of the order of $a_{COB} = 10.8 R_c$, where R_c is the radius of the Sun.

In (26) and in (27) it was found that a typical CMB radiation source has a radius of 0.68 pc and a mass of the order of. $31.2M_c$. The sources of radiation CIB and COB in (40-41) also have masses of the order of $31M_c$. It turns out that during cosmological evolution, CMB microwave radiation sources first become isolated in the form of gas clouds with a radius of the order of 0.68 pc. When these clouds are subsequently compressed by gravitational forces to a radius of the order of $a_{CIB} = 1136$ AU, protoplanetary systems containing gas and dust arise, leading to infrared background radiation CIB. The compression of clouds slows down due to the appearance of pressure in the gas, and the process of planet formation begins in the clouds. At the same time, the bulk of gas and dust in the center of each cloud continues to compress. As a result, primordial stars emerge, producing optical background radiation COB. Nuclear reactions begin in the depths of these stars, preventing the gravitational compression of matter. Thus, the CMB, CIB and COB emissions are associated with the most long-term and equilibrium phases in the evolution of primordial gas-dust clouds.

Since the masses of CIB and COB sources approximately coincide with the mass $m = 31.2M_c$ (27) of CMB sources, the concentration of CIB and COB sources in the early Universe approximately coincides with the concentration $n = \frac{\rho_b}{m} = 3.4\times10^{-60}$ m^{-3} (28) of CMB sources. Due to their large masses, primordial stars that are the sources of COB should transform into neutron stars. Thus, the concentration n can be considered as the concentration of primordial neutron stars. The average distance between such stars can be estimated using the formula $R_s = \frac{1}{\sqrt[3]{n}} \approx 6.7\times10^{19}$ m or $R_s \approx 2.16$ kpc. On the other hand, the observable Universe has a volume of the order of 3.6×10^{80} m^3, which contains about 10^{24} stars [38]. The concentration of stars in the Universe is on the order of 3.6×10^{-56} m^{-3}. Comparing the concentration of all stars with the concentration of primordial neutron stars leads to the fact that there are about 10^4 ordinary stars per a neutron star. This ratio of stars is indeed confirmed by observations.

Modern instruments allow us to measure angular power spectra not only for CMB, but also for CIB radiation [39]. Thus, the methods for analyzing the structure of radiating objects, developed in [30] for CMB, can also be applied to CIB radiation. According to [30], the mass density of the medium, which contains objects, clusters, and particles and is responsible for the appearance of CMB angular harmonics, equals 9×10^{-23} kg/m^3. This mass density does not exceed the mass density in (40-41) of the objects, which can be the sources of CIB and COB

radiation. This implies the possibility that the cause of harmonics in the CMB and CIB power spectra may be the same objects, clusters and particles located in the shells of the corresponding gas-dust clouds at different stages of compression of these clouds.

In (34) it was shown that the formula for the energy density of CMB $u_s = \frac{4\sigma T_s^4}{c} = 1.1\times10^{-13}$ J/m^3 (20), where $T_s = 3.472$ K is the temperature of CMB sources in the early Universe, cannot be applied to the entire Universe. Instead of u_s, a significantly lower average volumetric energy density of the CMB was calculated, equal to $\overline{u} = 1.4\times10^{-23}$ J/m^3 according to (33). This was because the gas mass m occupying the volume V in (34) in the initially homogeneous Universe with the mass density ρ_b, only after being compressed into a gas cloud with a volume V_s and density ρ_s. would start radiating like a black body with the temperature $T_s = 3.472$ K. As CMB photons move through space, their energy decreases due to cosmological redshift. In addition, photons interact with the matter of many CMB sources and are partially scattered. As a result, the intensity of the CMB radiation decreases, and the spectrum of CMB photons becomes close to the observed spectrum of the radiation of a black body with temperature $T = 2.7255$ K.

For CIB and COB radiation the situation is largely similar. As in the case of CMB radiation, CIB and COB radiation are nonequilibrium and for them there is no global blackbody consisting of matter and bounding the entire Universe. This means that in fact we always observe discrete sources of radiation, which at large distances merge into an almost uniform background.

9. Discussion of results

A well-known problem of the Big Bang theory in cosmology is the complete lack of understanding of the nature of such an explosion and of the origin of matter as such. The subsequent use of the general theory of relativity in the $\Lambda - CDM$ model adds new problems, such as singularities and metric space expansion, which are incomprehensible from the perspective of physics, the appearance of unidentified dark matter and mystical dark energy. The use of multiple fitting parameters in the $\Lambda - CDM$ model further undermines the credibility of the modern version of the Big Bang theory.

In [40], six fitting parameters are listed, and it is concluded that despite the accuracy of the results' fitting, it is still not enough to consider the $\Lambda - CDM$ model correct. In [13], the following conclusion was reached: "However, in cosmology, it has unfortunately been the case

that even a long series of failed predictions has not generally led to the rejection of theories, but rather to their unlimited modification with ad hoc hypotheses, such as inflation, non-baryonic matter, and dark energy."

It is noted in [41] that it could be possible to improve the situation with predictions in the $\Lambda - CDM$ model if, in addition to the seven fitting parameters of the model, we would assume, for example, the existence of early or dynamical dark energy, neutrino interactions, cosmological models with additional interactions, primordial magnetic fields, modified theories of gravitation, etc.

On the other hand, cosmology in the theory of infinite hierarchical nesting of matter finds the source and cause of origin of matter and the forms of its existence in the uniform evolutionary process of transformation of the main carriers at all matter levels [15]. This means, for example, that the evolution of the matter of planets and stars at the stellar level of matter is due to the evolution and action of carriers belonging to lower matter levels. Each matter level has its own main carrier as the most stable and balanced object, such as a neutron star, nucleon, praon, graon, etc., respectively. The similarity principle assumes the existence of the same coefficients of similarity in mass, size and speed of processes between the respective objects of the adjacent matter levels, which allows us to find the physical parameters of the main carriers of matter. As a consequence, a neutron star contains as many nucleons as each nucleon contains praons, and as each praon contains graons.

The main driving forces for matter evolution are electromagnetic and gravitational forces, which can be reduced to the action of carriers of the lowest matter levels, moving at relativistic speeds [10], [42-46]. This point of view is supported in [47] by the fact that the evolution of matter in the early Universe turns out to be little dependent on external factors and is determined mainly by internal factors.

It follows from the principle of similarity of matter levels that the analogs of a neutron star at the nucleon level of matter are nucleons, and the analogs of white dwarfs are the so-called nuons [4], which have the same mass range as nucleons. Nuons are similar in their properties to muons, but the origins of these particles are different: nuons appear similar to white dwarfs in the course of long-term evolution of matter, and muons appear mainly in the rapid decay of pions, while pions are assumed to be the analogs of low-mass and therefore unstable in the decay of neutron stars. Moreover, neutral nuons play the role of dark matter, which manifests itself through gravitational effects both on the motion of stars and gas clouds inside galaxies,

and on the motion of galaxies themselves during their interaction [48]. In contrast, the $\Lambda - CDM$ model has difficulties explaining dark matter, describing its evolution and origin.

The CMB generation process continues to occur today, although on a smaller scale. The properties of the coldest dark nebulae with masses up to $100M_c$ are quite close to those of primordial gas-dust clouds. Thus, practically opaque Bock globules, which are distinguished by their black color, have a temperature in the range from several degrees to 30 K and a typical mass of up to $30M_c$. From the standpoint of thermal radiation, such objects can model the properties of a blackbody quite well. Here, we provide as examples references to the spectra of the infrared sources IRS 1 and IRS 2 in [49-50] and to the spectrum of the Bock globule B335 in [51].

One review [52] described the properties of 248 small molecular clouds, most of which are Bok globules. It is assumed that in our Galaxy system the average distance between such globules is 600 pc, and the average mass of a globule is approximately $11M_c$. This distance can be compared with the value $R_s \approx 2.16$ kpc found for the distance between the primordial gas-dust clouds of the early Universe through the concentration n of CMB sources in (28).

According to [52], for most globules the radiation temperature of gas does not exceed 4.5 K, and the kinetic temperature does not exceed 8.5 K. Since globules are heated by radiation from the surrounding star background, the dust temperature in globules turns out to be higher than the gas temperature and depends on the measured frequency band and on the size of the dust particles. On average, the dust temperature is close to 25 K. Under such conditions, the spectrum of some globules appears to be not the blackbody spectrum at one fixed temperature, but rather the sum of the spectra of individual components consisting of gas and dust.

In [53], by analyzing the absorption lines of water molecules in a large cloud of water vapor near the HFLS3 galaxy, it was found that the temperature required for this exciting radiation ranges from 16.4 to 30.2 K. Since the HFLS3 galaxy has a redshift of the order of magnitude $z = 6.34$ and is located sufficiently far away, this temperature is considered from the point of view of the $\Lambda - CDM$ model as the CMB temperature at an earlier time. Moreover, due to the space expansion since then, the CMB temperature should have decreased to the current value of $T = 2.7255$ K.

On the other hand, radiation at a temperature ranging from 16.4 to 30.2 K is quite typical for gas clouds and Bok globules under the action of radiation from surrounding stars, including those in the most distant galaxies. In the model we are considering, the CMB temperature at the moment of emission coincides with the temperature $T_s = 3.472$ K (25) of gas-dust clouds

with masses on the order of $31M_c$, so distant from us that their redshift is much greater than the redshift of the observed galaxies.

How does the CMB radiation spectrum almost exactly correspond to the blackbody spectrum? Here, the following circumstances can be taken into account. First, we assume that there were no stars around the primordial gas-dust clouds of the early Universe that could noticeably heat the clouds and influence the form of the clouds' spectrum. Then, the spectrum of each cloud could be sufficiently close to the spectrum of a blackbody with the temperature $T_s = 3.472$ K.

Another circumstance is associated with the size of the visible Universe. Substituting in (8) the maximum measured value of redshift $z = 1089$ for the CMB according to [54] at $H = 70$ km/(s·Mpc), we find the radius of the visible Universe $r = 9.24 \times 10^{26}$ m or 30 Gpc. Light can travel this distance in $t = \frac{r}{c} = 98$ billion years. This time is less than the minimum compression time $t_{\min} \approx \sqrt{\frac{3\pi}{32G\rho_b}} = 145$ billion years, which was found according to (16) for the compression of all baryonic matter during the formation of the visible Universe.

It should be noted that when measuring CMB intensity, it is necessary to exclude radiation from bright point sources such as clusters of stars and galaxies from the obtained data to determine the background radiation precisely. However, the redshift of the most distant observable galaxies does not exceed $z = 12$. For example, the redshift of the galaxy GN-z11 equals $z = 11.09$ according to [55]. This redshift is significantly less than the redshift of the CMB, which reaches $z = 1089$. Thus, CMB radiation travels the main part of its way in unexplored distant regions of cosmic space.

In (6-7) the fact was used that the cross sections of CMB sources in the early Universe and the concentration of sources are such that at very large distances, these cross-sections begin to overlap each other; and, therefore, the Beer–Lambert law becomes valid. As a result, the CMB radiation coming to the Earth from distant sources has enough time to interact with the matter of multiple closer sources and additionally thermalize. This approach inevitably turns the CMB spectrum into an averaged spectrum that is close to the equilibrium spectrum of a blackbody.

The presented model is consistent with the results in [56], where the so-called virial gas clouds located in the halo of galaxies make it possible to explain the rotational anisotropy observed in the CMB. In [57], within the framework of the standard model of the expanding Universe, the evolution of virial clouds from the surface of the last scattering to the formation

of primordial stars of population III was considered. These virial clouds, which are also in thermal equilibrium with the CMB, as in our approach, have almost the same density as the primordial gas-dust clouds in our model. Thus, the conclusions in [56-57] concerning primordial gas-dust clouds prove our calculations.

The Earth and the Sun are known to move relative to the reference frame, in which the CMB is isotropic, at a speed of approximately 370 km/s. If we take into account the motion of the Sun in our galaxy and its motion in the Local Group of Galaxies, then the speed of the Local Group of Galaxies relative to the CMB's isotropic reference frame will be about $V_g = 627$ km/s [58]. In the $\Lambda - CDM$ model, the cosmological redshift is interpreted as a result of the Universe expansion, which has the mathematical meaning of a change in the spacetime metric, caused by an unknown factor. The physical meaning of this space expansion is an obvious subject for discussion regarding the justifiability of the use of mathematical hypotheses in the real physics of phenomena. It is assumed that at large distances from the Earth, galaxies and other objects, located there, are moving away from each other at tremendous speeds due to space expansion. These speeds can significantly exceed the speed V_g of motion of the Local Group of Galaxies relative to the isotropic reference frame of the CMB. So why from the entire speed spectrum do we observe a relatively small speed V_g, is it by chance?

From the viewpoint of the theory of infinite hierarchical nesting of matter, the answer lies in the fact that, for matter evolution and for the emergence of a new matter level with more massive objects, neither the Big Bang, nor the metric expansion of spacetime or high speeds of motion are needed. The deviation of the speed of galaxies and star clusters from the speed of the CMB's isotropic reference frame can be caused only by the gravitational action of galaxies on each other. When averaging the matter's speeds over the volume of the visible Universe, the obtained average speed must coincide with the speed of the CMB's reference frame because CMB occurs in the early Universe and, on average, is stationary relative to the global distribution of matter.

Taking this into account, the problem of space flatness on cosmological scales becomes understandable when even at very large distances, spacetime is practically not curved. Therefore, there is no great need to calculate any curved metric, which is always needed in the general theory of relativity, even in flat Minkowski spacetime. In this case, instead of the general theory of relativity, it is more convenient to use the covariant theory of gravitation [59-60], in which the metric effects are separated from the gravitational effects. This means that gravitation does not depend on a metric; rather, it is a real physical force, such as the

electromagnetic force, which exists even in Minkowski spacetime, when there is no spacetime curvature.

Paradoxes arising from the concept of space expansion were analyzed in [61], such as the violation of the law of conservation of energy for local comoving volumes, the Newtonian form of Friedmann's equations, the superluminal velocities of distant galaxies as a result of space expansion, and Hubble's law in inhomogeneous distributions of galaxies, etc. The main reason for the appearance of such paradoxes is the general theory of relativity due to the absence of the energy-momentum tensor of the gravitational field in this theory, which casts doubt on the possibility of using this theory in cosmology.

It was noted in [62] that the time scale in the $\Lambda - CDM$ model does not correspond to the time, which was required for the formation of large galactic clusters and voids in the early Universe. In this regard, it is assumed that this discrepancy may be due to the use of the general theory of relativity, which should be replaced with another gravitation theory, for example, modified Newtonian dynamics (MOND). The authors of [62] draw the following conclusion from their article: at the present moment, we understand neither the distribution of matter and energy in the Universe nor the law of gravitation, which governs this.

It was found in [63] that a supercluster of galaxies with a radius of about 6 Mpc rotated at an angular velocity ω equal to 2°.9 degrees per 10 billion years, or $\omega = 1.6 \times 10^{-19}$ s^{-1}. According to [64], large galactic clusters with sizes on the order of $R_c \approx 800$ Mpc can experience general motion at velocities up to $V_c \approx 1000$ km/s. Assuming that this motion arises from rotation, for the angular velocity in the first approximation, we have $\omega_c \approx \frac{V_c}{R_c} \approx 4 \times 10^{-20}$ s^{-1}. The large-scale structure of the Universe has the form of a cosmic web and consists of individual filaments that contain galactic clusters. The difference ΔV in the linear velocity of rotation of different points in the filaments can reach 100 km/s at a distance ΔR between the points equal to 1 Mpc, which gives an estimate of the angular velocity of rotation $\omega_f \approx \frac{\Delta V}{\Delta R} \approx 3 \times 10^{-18}$ s^{-1} according to [65].

If we assume that the entire visible Universe also rotates, then its limiting rotation can be estimated by the formula for the first cosmic velocity, assuming that the matter at the edge of the Universe is in equilibrium between the gravitational force and the centripetal force:

$$\omega_U = \sqrt{\frac{GM_U}{R_U^3}} = \sqrt{\frac{4\pi G\rho_U}{3}} .$$

where M_U, R_U and ρ_U denote the mass, radius and mass density of the Universe, respectively. Substituting here the mass density $\rho_b = 2.1\times10^{-28}$ kg/m^3 instead of ρ_U, we find $\omega_U = 2.4\times10^{-19}$ s^{-1}, which has the same order of magnitude with respect to the rotation of large galactic structures. This rotation corresponds to a period of approximately 830 billion years.

It is obvious that any general rotation of the observable Universe contradicts the Big Bang since, due to rotation the Universe would have a nonzero angular momentum. In the scenario of the Big Bang and subsequent inflation up to the state of the observable Universe, it turns out that, taking into account the law of conservation of angular momentum, the object that gave rise to the Universe should have had an enormous angular momentum for its small size, which seems completely improbable. At the same time, in the hierarchical model, the object, from which the early Universe was formed could consist of a huge cloud of praons. If this cloud with the sizes of the order of the observable Universe had any general rotation, then the emerging Universe would have the same rotation after the evolution of praonic matter and its transformation into nucleons and nuons.

We believe that other, less complex cosmological problems can also find their solution within the framework of the theory of infinite hierarchical nesting of matter and a stationary Universe. For example, in [66] it is indicated that expansion of space is not required to explain the change in luminosity in the spectra of supernovae. Thus, cosmology can be constructed with a minimum of assumptions and paradoxical conclusions that contradict the traditional logic of physics.

10. Conclusions

Cosmic microwave background radiation (CMB) along with the effect of the cosmological redshift of radiation spectra are usually considered phenomena that find an acceptable explanation within the framework of the Big Bang theory. Indeed, these phenomena are rather difficult to explain, which eventually led to the idea of the Big Bang. However, due to the significant drawbacks of this theory, which are described above, we consider this theory to be too exotic and radical and suggest another explanation for emergence of CMB.

In our approach, the necessary source of CMB energy turns out to be gravitational energy, which, under matter clustering in primordial gas-dust clouds in the early Universe, is released

in the form of the kinetic energy of motion of matter particles, according to the virial theorem. The subsequent collisions of particles convert kinetic energy into thermal energy, heating the particles, so that gas-dust clouds can radiate as black bodies at the temperature $T_s = 3.472$ K (25). During the time until CMB radiation from distant regions of the Universe reaches the Earth, the temperature of this radiation decreases to the value $T = 2.7255$ K.

Based on this approach, we first find formula (7) for the volumetric power L of CMB energy generation in cosmic space, and then we find the main characteristics of primordial gas-dust clouds, including their radius $a \approx 0.68$ pc (26), mass $m \approx 31 M_c$ (27), volume concentration of clouds $n \approx 3.4 \times 10^{-60}$ m^{-3} (28) and distance between neighboring clouds $R_s \approx 2.2$ kpc. For the volumetric power L of CMB energy generation, the value $L \approx 1.5 \times 10^{-31}$ W/m^3 (29) is obtained, while the generation power per nucleon of a typical gas-dust cloud, as well as per nucleon in the early Universe, is equal to $\frac{L}{n_b} \approx 1.2 \times 10^{-30}$ W/nucleon (30).

We can conclude that the CMB originated as thermal radiation from primordial gas-dust clouds. This thermal radiation could interact with a large number of particles in each cloud, which, in view of the slowly changing equilibrium state of the clouds and their opacity and weak reflection, provides the CMB radiation spectrum close to that of blackbody radiation. In addition, CMB radiation coming from very large distances passes through many separate CMB sources in the form of gas clouds on its way to Earth. This further contributes to the transformation of the CMB spectrum into a blackbody spectrum.

As indicated in Section 6 with reference to [30], the angular harmonics in the CMB power spectrum can be explained if we take into account matter clustering near the surface of primordial gas-dust clouds. This possibility is supported by the presence of both small and large dust particles observed in Bok globules, leading to significant polarization of radiation in the millimeter range [67-69] up to values on the order of 10 % or more. In this regard, the degree of polarization of the CMB is also approximately 10 %. Thus, the primordial gas-dust clouds generating CMB during their evolution could take the form of globules.

In addition to CMB, the approach under consideration can be applied to infrared background radiation (CIB) and optical background radiation (COB). The estimates made in Section 7 give reason to believe that the CIB emission could have originated in protoplanetary clouds, while the contribution to the COB emission was made by primordial stars.

Although the blackbody CMB radiation coming to the Earth from all directions has an intensity $I = \sigma T^4$, this does not mean that the ubiquitous occurrence of CMB energy density

in cosmic space is equal to $u = \frac{4\sigma T^4}{c} = 4.17 \times 10^{-14}$ J/m^3, similar to blackbody radiation. As shown in (33), the average CMB energy density in the Universe should equal $\bar{u} = 1.4 \times 10^{-23}$ J/m^3. This happens because the CMB is radiation that is not in equilibrium with the global blackbody. Indeed, all CMB sources cannot form a closed surface entirely surrounding the radiation of the Universe, which is a necessary condition for the validity of the formula $u = \frac{4\sigma T^4}{c}$. The same applies to CIB radiation and COB radiation, which are also nonequilibrium.

Due to the difference between the energy density $\bar{u}$ and the energy density u_s (20) of blackbody radiation, it becomes possible to move away from the model of the hot expanding Universe. It follows from this model that the CMB energy density is equal to u everywhere, so that the ratio of the number of photons to the number of nucleons is equal to $\frac{n_f}{n_b} = \frac{n_f m_p}{\rho_b} = 3.3 \times 10^9$, which is close in magnitude to the ratio of volumes $\frac{V}{V_s}$ in (34). In our approach, the energy density $\bar{u}$ corresponds to the condition of practically the same number of photons and nucleons, which does not lead to the problem of excess photons over nucleons or to the need to introduce the hot Universe model.

Statements and declarations

The authors have no relevant financial or non-financial interests to disclose.

Data availability

The data underlying this article are available in the article and in its online supplementary material.

References

1. Flandern T.V. The Top 30 Problems with the Big Bang. Apeiron, Vol. 9 (2), pp. 72-90 (2002).

2. Narlikar J.V., Burbidge G. and Vishwakarma R.G. Cosmology and Cosmogony in a Cyclic Universe. Journal of Astrophysics and Astronomy, Vol. 28, pp. 67-99 (2007). http://dx.doi.org/10.1007/s12036-007-0007-5.

3. Gupta S.N.P. Uniformity of CMB in our Dynamic Universe. Journal of Astrophysics & Aerospace Technology, Vol. 4, Issue 1, 128 (2016). http://dx.doi.org/10.4172/2329-6542.1000128.

4. Fedosin S.G. Cosmic Red Shift, Microwave Background, and New Particles. Galilean Electrodynamics, Vol. 23, Special Issues No. 1, pp. 3-13 (2012). http://dx.doi.org/10.5281/zenodo.890806.

5. Millette P.A. On Eddington's Temperature of Interstellar Space and the Cosmic Microwave Background Radiation. Letters to Progress in Physics, Vol. 17, Issue 2, pp. 216-217 (2021).

6. Burbidge G. and Hoyle F. The Origin of Helium and the Other Light Elements. The Astrophysical Journal Letters, Vol. 509. L1-L3 (1998).

7. Hill R., Masui K.W., Scott D. The Spectrum of the Universe. Applied Spectroscopy, Vol. 72, Issue 5, pp. 663-688 (2018). https://doi.org/10.1177/0003702818767133. 1802.03694.pdf (arxiv.org)

8. Driver S.P. Measuring energy production in the Universe over all wavelengths and all time. Invited review for IAU Symposium 355, The Realm of the Low-Surface-brightness Universe, (eds: D. Valls-Gabaud, I. Trujillo & S. Okamoto) (2021). arXiv:2102.12089.

9. Fedosin S.G. The generalized Poynting theorem for the general field and solution of the 4/3 problem. International Frontier Science Letters, Vol. 14, pp. 19-40 (2019). https://doi.org/10.18052/www.scipress.com/IFSL.14.19.

10. Fedosin S.G. On the structure of the force field in electro gravitational vacuum. Canadian Journal of Pure and Applied Sciences, Vol. 15, No. 1, pp. 5125-5131 (2021). http://doi.org/10.5281/zenodo.4515206.

11. Ashmore L. Calculating the redshifts of distant galaxies from first principles by the new tired light theory (NTL). Vigier 11 conference in Liege, Belgium, August 2018. https://www.researchgate.net/publication/330005846_Calculating_the_redshifts_of_distant_galaxies_from_first_principles_by_the_new_tired_light_theory_NTL .

12. Ashmore L.A Relationship between Dispersion Measure and Redshift Derived in Terms of New Tired Light. Journal of High Energy Physics, Gravitation and Cosmology, Vol. 2, No. 4, Paper ID 70089, 19 pages (2016). https://doi.org/10.4236/jhepgc.2016.24045.

13. Lerner E.J. Observations contradict galaxy size and surface brightness predictions that are based on the expanding universe hypothesis. Monthly Notices of the Royal Astronomical Society, Vol. 477, pp. 3185-3196 (2018). https://doi.org/10.1093/mnras/sty728.

14. Lerner E.J., Falomo R., Scarpa R. UV surface brightness of galaxies from the local Universe to z ~ 5. International Journal of Modern Physics D, Vol. 23, No. 6, 1450058 (2014). https://doi.org/10.1142/S0218271814500588.

15. Sergey Fedosin (2014). The physical theories and infinite hierarchical nesting of matter. Volume 1, LAP LAMBERT Academic Publishing, pages: 580, ISBN 978-3-659-57301-9.

16. Hinshaw G.F., et al. Nine-Year Wilkinson Microwave Anisotropy Probe (WMAP) Observations: Cosmological Parameter Results. ApJS., Vol. 208, No. 2 19H. (2013). https://doi.org/10.1088/0067-0049/208/2/19.

17. Oldershaw R.L. The Self-similar Cosmological Paradigm: A New Test and Two New Predictions. Astrophysical Journal, Vol. 322, pp. 34-36 (1987). https://doi.org/10.1086/165699.

18. Oldershaw R.L. Self-Similar Cosmological model: Introduction and empirical tests. International Journal of Theoretical Physics, Vol. 28 (6), pp. 669-694 (1989). https://doi.org/10.1007/BF00669984.

19. Oldershaw R.L. Self-similar cosmological model: Technical details, predictions, unresolved issues, and implications. International Journal of Theoretical Physics, Vol. 28 (12), pp. 1503-1532 (1989). https://doi.org/10.1007/BF00671591.

20. Oldershaw R.L. Hierarchical cosmology. Astrophysics and Space Science, Vol. 189, pp. 163-168 (1992). https://doi.org/10.1007/BF00642965.

21. Fedosin S.G. Scale dimension as the fifth dimension of spacetime. Turkish Journal of Physics, Vol. 36, No. 3, pp. 461-464 (2012). http://dx.doi.org/10.3906/fiz-1110-20.

22. Shklovsky I.S. Stars: Their Birth, Life, Death. San Francisco, 1978, ISBN 0-7167-0024-7.

23. Edward Kolb and Michael Turner (1988). The Early Universe. Addison-Wesley. ISBN 978-0-201-11604-5.

24. Fedosin S.G. The virial theorem and the kinetic energy of particles of a macroscopic system in the general field concept. Continuum Mechanics and Thermodynamics, Vol. 29, Issue 2, pp. 361-371 (2017). https://dx.doi.org/10.1007/s00161-016-0536-8.

25. Fedosin S.G. The integral theorem of generalized virial in the relativistic uniform model. Continuum Mechanics and Thermodynamics, Vol. 31, Issue 3, pp. 627-638 (2019). http://dx.doi.org/10.1007/s00161-018-0715-x.

26. Fedosin S.G. The binding energy and the total energy of a macroscopic body in the relativistic uniform model. Middle East Journal of Science, Vol. 5, Issue 1, pp. 46-62 (2019). http://dx.doi.org/10.23884/mejs.2019.5.1.06.

27. Sievers J.L. et al. Cosmological Parameters from Cosmic Background Imager Observations and Comparisons with BOOMERANG, DASI, and MAXIMA. Astrophysical Journal, Vol. 591, No. 2, pp. 599-622 (2003). http://dx.doi.org/10.1086/375510.

28. Hu W, and Dodelson S. Cosmic Microwave Background Anisotropies. Annu. Rev. Astron. and Astrophys. Vol. 40, pp. 1-50 (2002). https://doi.org/10.1146/annurev.astro.40.060401.093926.

29. P.A. Zyla et al. (Particle Data Group). Review of Particle Physics. Progress of Theoretical and Experimental Physics, Vol. 2020, Issue 8, 083C01 (2020). https://doi.org/10.1093%2Fptep%2Fptaa104. Cosmic Microwave Background review by Scott and Smoot.

30. Červinka L. Transformation of the Angular Power Spectrum of the Cosmic Microwave Background (CMB) Radiation into Reciprocal Spaces and Consequences of This Approach. Journal of Modern Physics, Vol. 2, No. 11, pp. 1331-1347 (2011). http://dx.doi.org/10.4236/jmp.2011.211165.

31. Jeans J.H. The Stability of a Spherical Nebula. Philosophical Transactions of the Royal Society of London. Series A, Containing Papers of a Mathematical or Physical Character. Vol. 199, pp. 1-53 (1902).

32. Cabré A., Gaztañaga E., Manera M., Fosalba P., Castander F. Cross-correlation of Wilkinson Microwave Anisotropy Probe third-year data and the Sloan Digital Sky Survey DR4 galaxy survey: new evidence for dark energy. Monthly Notices of the Royal Astronomical Society: Letters, Vol. 372, Issue 1, pp L23–L27 (2006). https://doi.org/10.1111/j.1745-3933.2006.00218.x.

33. Pietrobon D., Balbi A., and Marinucci D. Integrated Sachs-Wolfe effect from the cross correlation of WMAP 3 year and the NRAO VLA sky survey data: New results and constraints on dark energy. Phys. Rev. D, Vol. 74, 043524 (2006). https://doi.org/10.1103/PhysRevD.74.043524.

34. Cruz M., Martinez-Gonzalez E., Vielva P., Cayon L. Detection of a non-Gaussian spot in WMAP. Monthly Notices of the Royal Astronomical Society, Vol. 356, Issue 1, pp. 29-40 (2005). https://doi.org/10.1111/j.1365-2966.2004.08419.x2005.

35. Mackenzie, Ruari; et al. Evidence against a supervoid causing the CMB Cold Spot. Monthly Notices of the Royal Astronomical Society. Vol. 470 (2), pp. 2328-2338 (2017). https://doi.org/10.1093/mnras/stx931.

36. Kopylov A.I.; Kopylova F.G. Search for streaming motion of galaxy clusters around the Giant Void. Astronomy & Astrophysics, Vol. 382 (2), pp. 389-396(2002). https://doi.org/10.1051/0004-6361:20011500.

37. Dominik J. Schwarz et al. CMB anomalies after Planck. Class. Quantum Grav. Vol. 33, No. 18, 184001 (2016). https://doi.org/10.1088/0264-9381/33/18/184001.

38. Marov M.Y. The Structure of the Universe. The Fundamentals of Modern Astrophysics. pp. 279-294 (2015). https://doi.org/10.1007%2F978-1-4614-8730-2_10. ISBN 978-1-4614-8729-6.

39. Maniyar A.S., Lagache G., Béthermin M. and Ilić S. Constraining cosmology with the cosmic microwave and infrared backgrounds correlation. A&A. Vol. 621, A32 (2019). https://doi.org/10.1051/0004-6361/201833765.

40. Debono I. and Smoot G.F. General Relativity and Cosmology: Unsolved Questions and Future Directions. Universe, Vol, 2(4), pp. 23 (2016). https://doi.org/10.3390/universe2040023.

41. Eleonora Di Valentino et al. In the realm of the Hubble tension - a review of solutions. Classical and Quantum Gravity, Vol. 38, No 15, 153001 (2021). https://doi.org/10.1088/1361-6382/ac086d.

42. Fedosin S.G. The graviton field as the source of mass and gravitational force in the modernized Le Sage's model. Physical Science International Journal, Vol. 8, Issue 4, pp. 1-18 (2015). http://dx.doi.org/10.9734/PSIJ/2015/22197.

43. Fedosin S.G. The force vacuum field as an alternative to the ether and quantum vacuum. WSEAS Transactions on Applied and Theoretical Mechanics, Vol. 10, Art. #3, pp. 31-38 (2015). http://dx.doi.org/10.5281/zenodo.888979.

44. Fedosin S.G. The charged component of the vacuum field as the source of electric force in the modernized Le Sage's model. Journal of Fundamental and Applied Sciences, Vol. 8, No. 3, pp. 971-1020 (2016). http://dx.doi.org/10.4314/jfas.v8i3.18.

45. Fedosin S.G. The substantial model of the photon. Journal of Fundamental and Applied Sciences, Vol. 9, No. 1, pp. 411-467 (2017). http://dx.doi.org/10.4314/jfas.v9i1.25.

46. Fedosin S.G. The principle of operation of an engine that draws energy from the electrogravitational vacuum. Jordan Journal of Physics, Vol. 17, No 1, pp. 87-95 (2024). https://doi.org/10.47011/17.1.8.

47. Tomoko L Suzuki et al. Extended star-forming regions within galaxies in a dense proto-cluster core at z = 2.53. Publications of the Astronomical Society of Japan, Vol. 71, Issue 4, 69 (2019). https://doi.org/10.1093/pasj/psz047.

48. Douglas Clowe et al. A Direct Empirical Proof of the Existence of Dark Matter. The Astrophysical Journal, Vol. 648, No. 2, L109 (2006). https://doi.org/10.1086/508162.

49. Beichman C.A. et al. The formation of Solar-type stars: IRAS observations of the dark cloud Barnard 5. Astrophysical Journal letters, Vol. 278, pp. 145-148 (1984).

50. Beichman C.A. et al. Candidate Solar-type protostars in nearby molecular cloud cores. Astrophysical Journal, Vol. 307, pp. 337-349 (1986).

51. Keene J. et al. Far-infrared detection of low-luminosity star formation in the Bok globule B335. Astrophysical Journal letters, Vol. 274, pp. 143-147 (1983).

52. Clemens D.P., Yun J.L., Heyer M.H. Bok globules and small molecular clouds - Deep *IRAS* photometry and ^{12}CO spectroscopy. Astrophysical Journal Supplement. Vol. 75, pp. 877-904 (1991). https://doi.org/10.1086/191552.

53. Riechers D. et al. Microwave Background Temperature at Redshift 6.34 from H2O Absorption. Nature, Vol. 602, pp. 58-62 (2022). https://doi.org/10.1038/s41586-021-04294-5.

54. Lineweaver C., Davis T.M. Misconceptions about the Big Bang. Scientific American. Vol. 292 (3): pp. 36-45 (2005). https://doi.org/10.1038/scientificamerican0305-36.

55. Oesch P.A., Brammer G., van Dokkum P. et al. A Remarkably Luminous Galaxy at z=11.1 Measured with Hubble Space Telescope Grism Spectroscopy. The Astrophysical Journal, Vol. 819 (2), pp.129 (2016). https://doi.org/10.3847/0004-637X/819/2/129.

56. Qadir A., Tahir N. and Sakhi M. Virial clouds explaining the observed rotational asymmetry in the galactic halos. Physical Review D, Vol.100, No. 4, 043028 (2019). http://dx.doi.org/10.1103/PhysRevD.100.043028.

57. Tahir N., Qadir A., Sakhi M. et al. Evolution of virial clouds-I: From the surface of last scattering up to the formation of population-III stars. Europ. Phys. J. C. Vol. 81, 827 (2021). https://doi.org/10.1140/epjc/s10052-021-09620-9.

58. Kogut A. et al. Dipole Anisotropy in the COBE Differential Microwave Radiometers First-Year Sky Maps. The Astrophysical Journal, Vol. 419, pp. 1-6 (1993). http://doi.org/10.1086/173453.

59. Fedosin S.G. The Pioneer Anomaly in Covariant Theory of Gravitation. Canadian Journal of Physics, Vol. 93, No. 11, pp. 1335-1342 (2015). http://dx.doi.org/10.1139/cjp-2015-0134.

60. Fedosin S.G. The Gravitational Field in the Relativistic Uniform Model within the Framework of the Covariant Theory of Gravitation. International Letters of Chemistry, Physics

and Astronomy, Vol. 78, pp. 39-50 (2018). http://dx.doi.org/10.18052/www.scipress.com/ILCPA.78.39.

61. Baryshev Y. Conceptual Problems of the Standard Cosmological Model. AIP Conference Proceedings, Vol. 822, pp. 23 (2006); https://doi.org/10.1063/1.2189119.

62. Asencio E., Banik I., Kroupa P. A massive blow for ΛCDM − the high redshift, mass, and collision velocity of the interacting galaxy cluster El Gordo contradicts concordance cosmology. Monthly Notices of the Royal Astronomical Society, Vol. 500, Issue 4, pp. 5249-5267 (2021). https://doi.org/10.1093/mnras/staa3441.

63. Joon Hyeop Lee et al. Mysterious Coherence in Several-megaparsec Scales between Galaxy Rotation and Neighbor Motion. The Astrophysical Journal, Vol. 884, No. 2, pp. 104-119 (2019). https://doi.org/10.3847/1538-4357/ab3fa3.

64. Salehi A., Yarahmadi M., Fathi S. The cosmological bulk flow in QCDM model: (In)consistency with ΛCDM. Monthly Notices of the Royal Astronomical Society, Volume 504, Issue 1, June 2021, Pages 1304–1319, https://doi.org/10.1093/mnras/stab909.

65. Wang P., Libeskind N.I., Tempel E. et al. Possible observational evidence for cosmic filament spin. Nature Astronomy, Vol. 5, pp. 839-845 (2021). https://doi.org/10.1038/s41550-021-01380-6.

66. Crawford D.F. A problem with the analysis of type Ia supernovae. Open Astronomy, Vol. 26, No. 1, pp. 111-119 (2017). https://doi.org/10.1515/astro-2017-0013.

67. Ward-Thompson D., Kirk J.M., Crutcher R.M., Greaves J.S., Holland W.S., Andre P. First observations of the magnetic field geometry in prestellar cores. The Astrophysical Journal, Vol. 537, L135 (2000). https://doi.org/10.1086/312764.

68. Matthews B.C., Wilson C.D. Magnetic fields in star-forming molecular clouds. V. Submillimeter polarization of the Barnard 1 dark cloud. The Astrophysical Journal, Vol. 574. pp. 822-833 (2002). https://doi.org/10.1086/341111.

69. Zielinski N., Wolf S. and Brunngräber R. Constraining the magnetic field properties of Bok globule B335 using SOFIA/HAWC+. A&A, Vol. 645, A125 (2021). https://doi.org/10.1051/0004-6361/202039126.